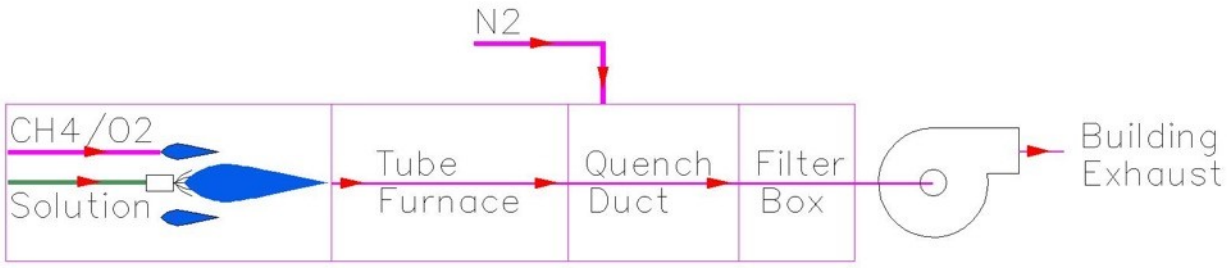

Figure S1. Simplified schematic of the flame spray pyrolysis apparatus.

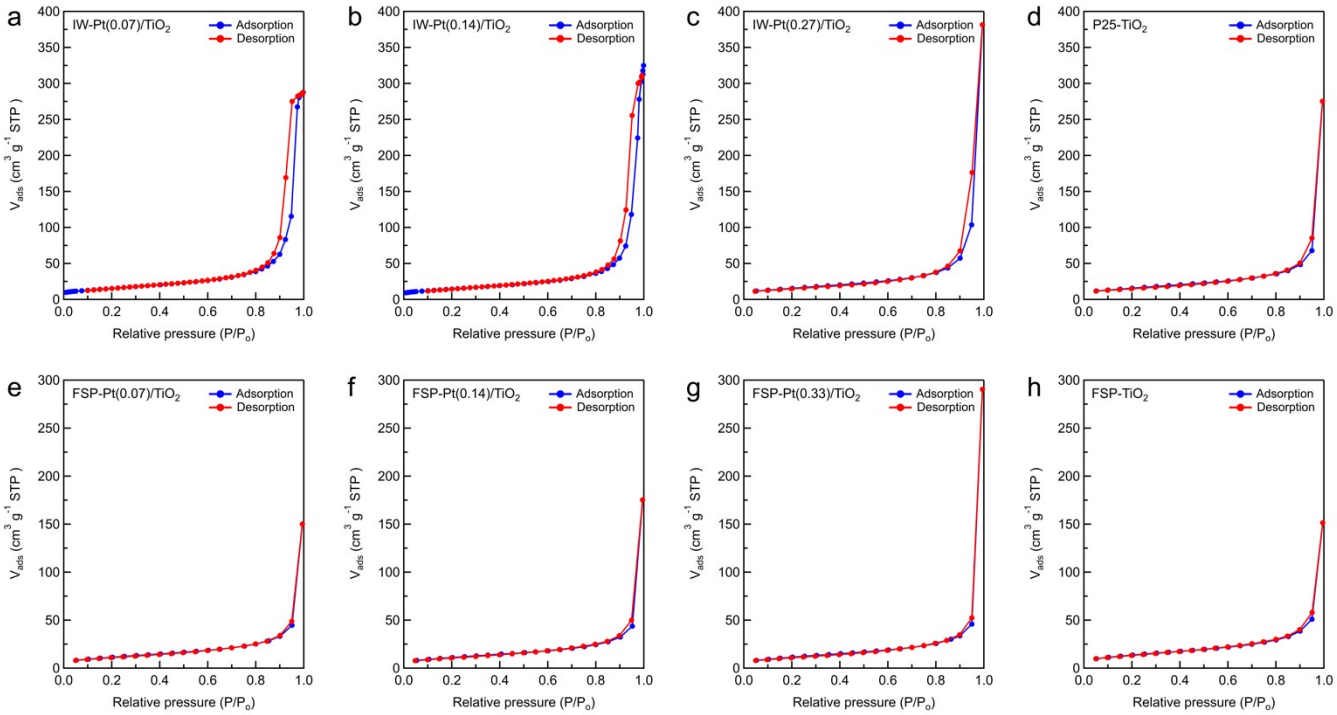

Figure S2. BET isotherms for Pt/TiO_2 catalysts prepared using flame spray pyrolysis (FSP) at (a) 0.07, (b) 0.14, (c) 0.33, and (d) 0 weight % Pt and incipient wetness (IW) at (e) 0.07, (f) 0.14, (g) 0.27, and 0 weight % Pt.

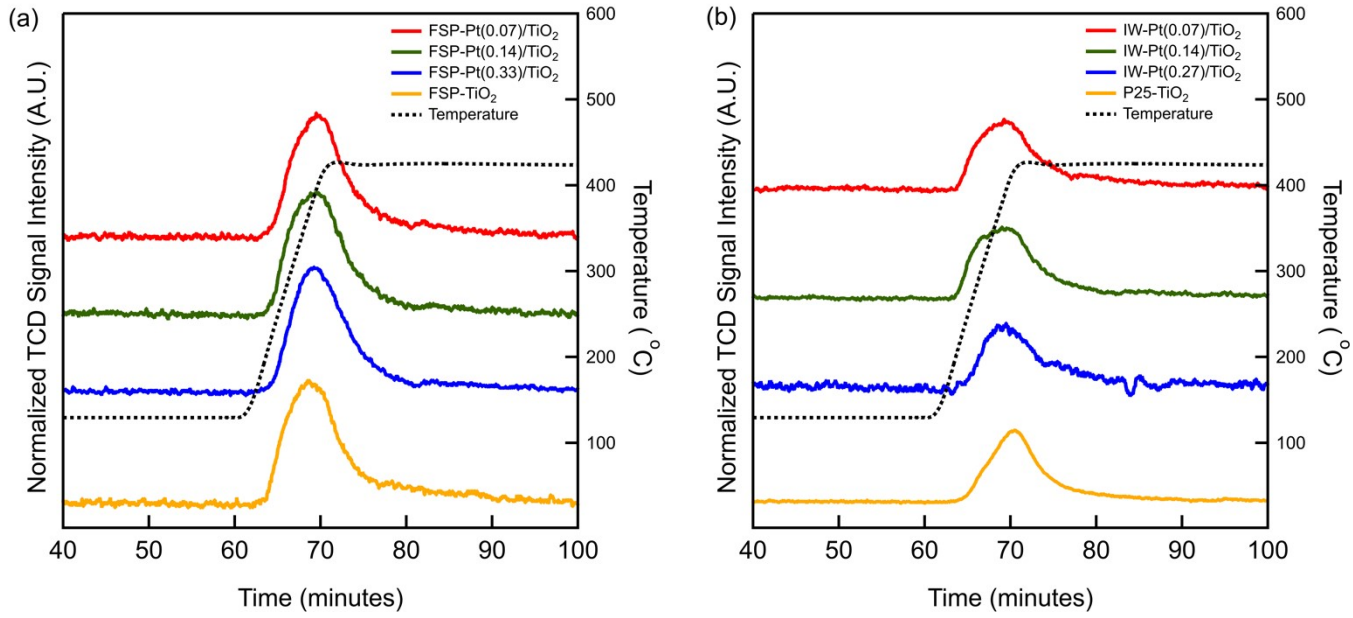

Figure S3. NH_3-TPD profiles for Pt/TiO_2 catalysts prepared using (a) FSP and (b) IW methods

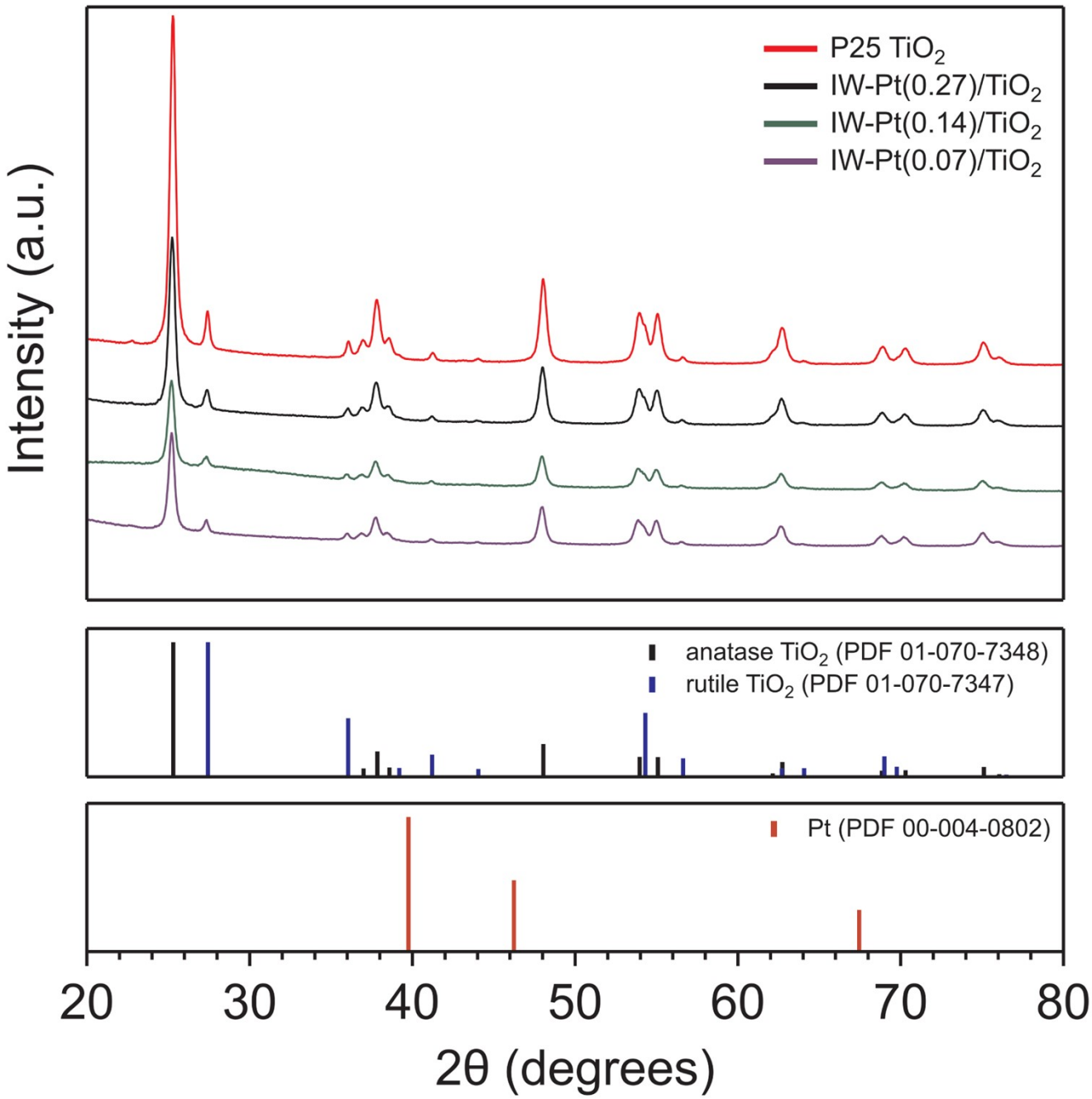

Figure S4. XRD patterns of IW-derived Pt/TiO_2 and TiO_2 with reference patterns provided below.

Table S1. Pore volume and pore size of Pt/TiO_2 catalysts and control materials as determined by N_2 physisorption

Catalyst	Pore volume ($cm^3 \cdot g^{-1}$)	Average pore size (nm)
FSP-TiO_2	0.24	10
P25-TiO_2	0.43	15
FSP-Pt(0.07)/TiO_2	0.23	11
FSP-Pt(0.14)/TiO_2	0.27	13
FSP-Pt(0.33)/TiO_2	0.45	21
IW-Pt(0.07)/TiO_2	0.44	33
IW-Pt(0.14)/TiO_2	0.47	36
IW-Pt(0.27)/TiO_2	0.59	21

Table S2. Mass % of rutile and anatase titania phases as determined by the RIR method and their respective crystallite sizes by Scherrer analysis for all FSP-Pt/TiO_2, IW-Pt/TiO_2 catalysts and their bare FSP-TiO_2 and P25-TiO_2 analogues.

Material	Anatase (mass%)	Anatase Crystallite Size (nm, XRD)	Rutile (mass%)	Rutile Crystallite Size (nm, XRD)
FSP-TiO_2	81.7	28.9(4)	18.3	37.9(30)
P25–TiO_2	92.5	19.84(1)	7.5	29.3(5)
FSP-Pt(0.07)/TiO_2	84.6	26.1(3)	15.4	33.4(20)
FSP-Pt(0.14)/TiO_2	85.2	31.4(5)	14.8	34.8(26)
FSP-Pt(0.33)/TiO_2	83.8	33.6(4)	16.2	43.0(41)
IW-Pt(0.07)/TiO_2	91.3	19.07(16)	8.7	28.2(13)
IW-Pt(0.14)/TiO_2	92.1	17.59(16)	7.9	23.9(15)
IW-Pt(0.27)/TiO_2	92.5	18.20(12)	7.5	24.4(6)

Table S3. STEM determined average Pt particle sizes for all FSP- and IW-Pt/TiO_2 catalysts.

Material	Pt Crystallize Size (nm, S/TEM)
FSP-Pt(0.07)/TiO_2	n.d.
(reduced)FSP-Pt(0.07)/TiO_2	1.1 ± 0.2
FSP-Pt(0.14)/TiO_2	0.5 ± 0.2
(reduced)FSP-Pt(0.14)/TiO_2	1.5 ± 0.7
FSP-Pt(0.33)/TiO_2	0.8 ± 0.2
(reduced)FSP-Pt(0.30)/TiO_2	1.3± 0.4
IW-Pt(0.07)/TiO_2	0.9 ± 0.2
IW-Pt(0.14)/TiO_2	1.1 ± 0.2
IW-Pt(0.27)/TiO_2	1.3 ± 0.5

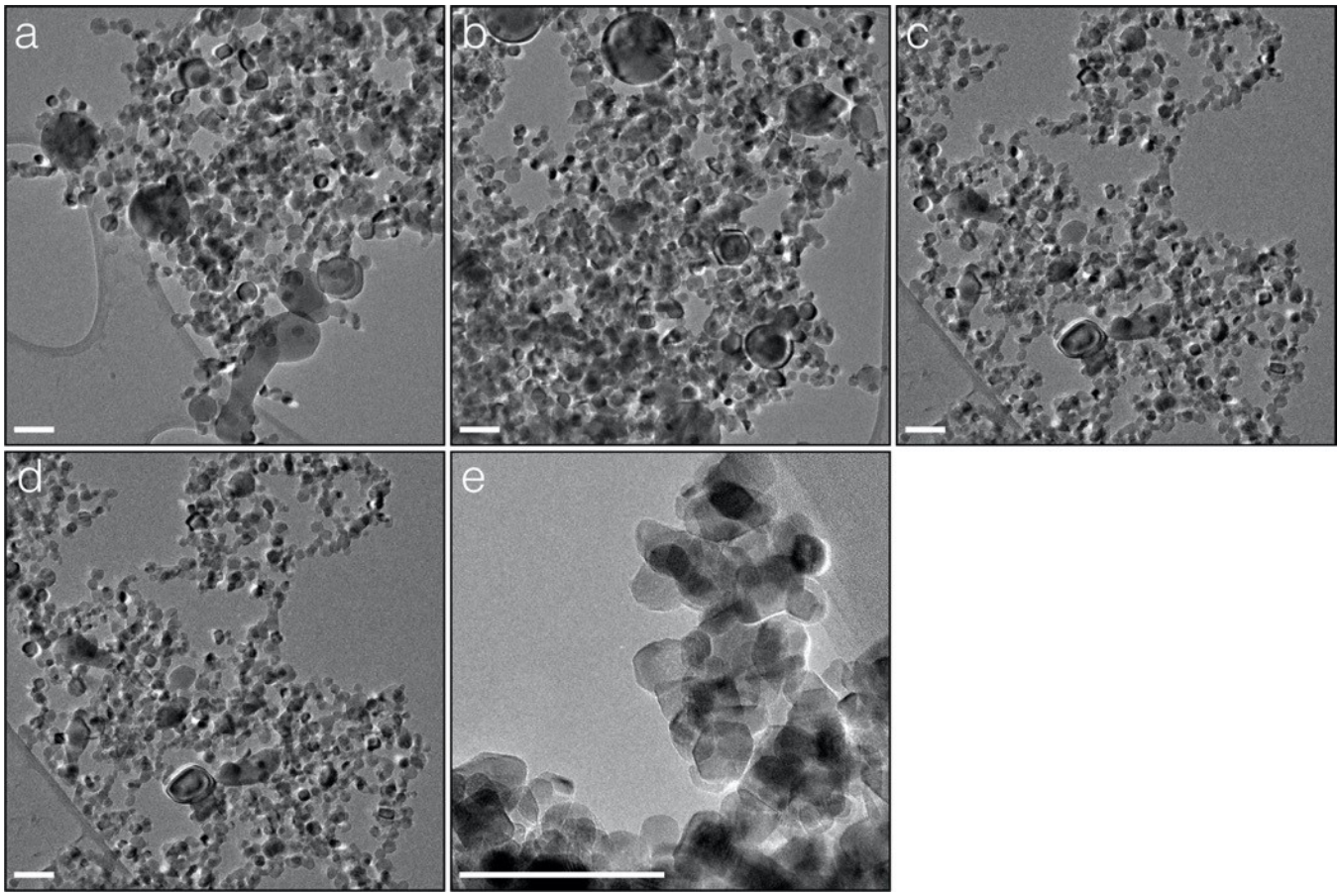

Figure S5. TEM images of (a) FSP-Pt(0.07)/TiO_2, (b) FSP-Pt(0.14)/TiO_2, (c) FSP-Pt(0.33)/TiO_2, (d) FSP-TiO_2, and (e) P25-TiO_2. All scale bars are 100 nm.

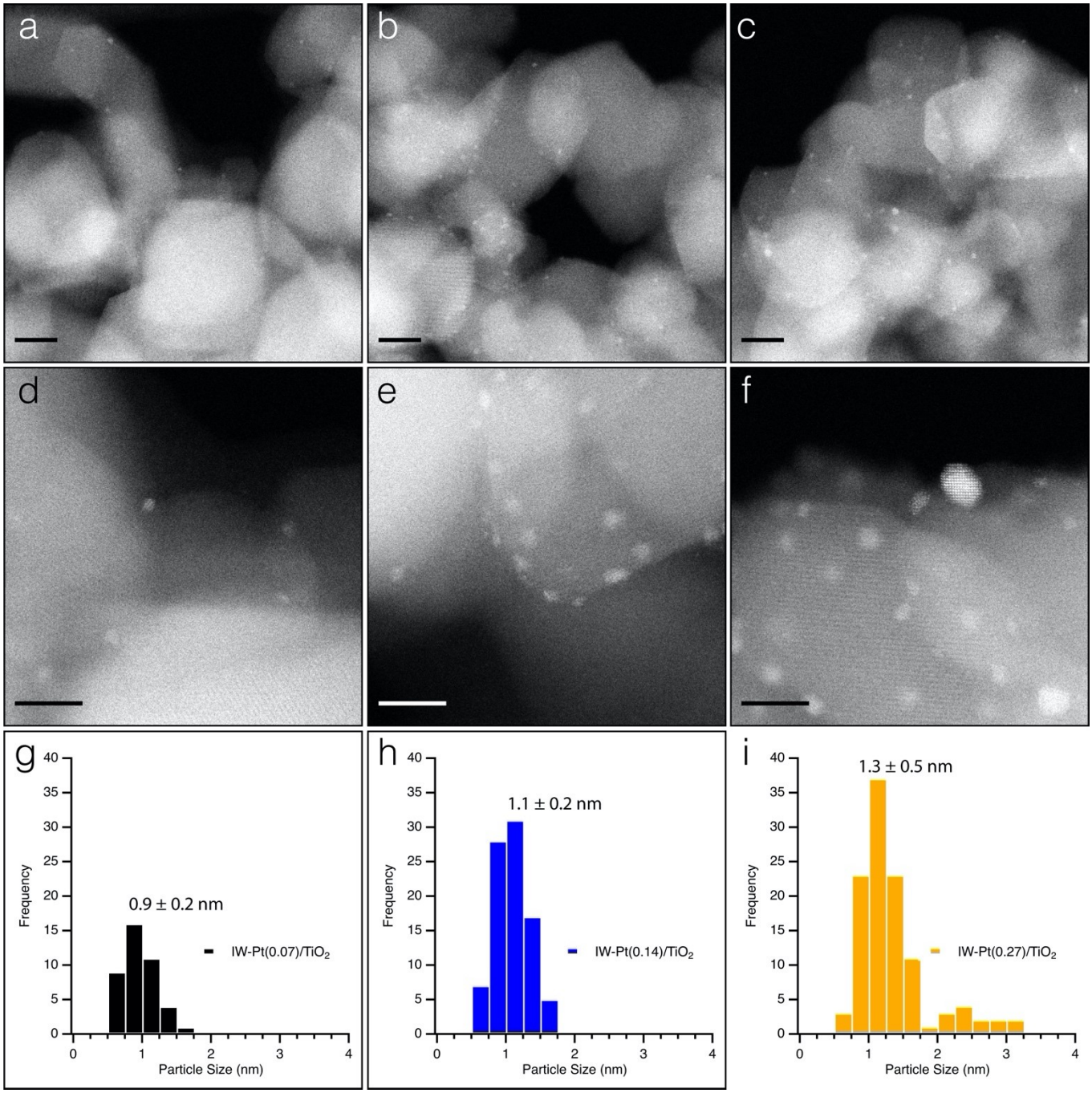

Figure S6. Low-magnification HAADF-STEM images of (a) IW-Pt(0.07)/TiO_2, (b) IW–Pt(0.14)/TiO_2, and (c) IW-Pt(0.27)/TiO_2 and high-magnification HAADF-STEM images of (d) IW-Pt(0.07)/TiO_2, (e) IW–Pt(0.14)/TiO_2, and (f) IW-Pt(0.27)/TiO_2. Scale bars for a-c are 10 nm and for d-f are 5 nm. Particle size histograms for (g) IW-Pt(0.07)/TiO_2, (h) IW–Pt(0.14)/TiO_2, and (i) IW-Pt(0.27)/TiO_2.

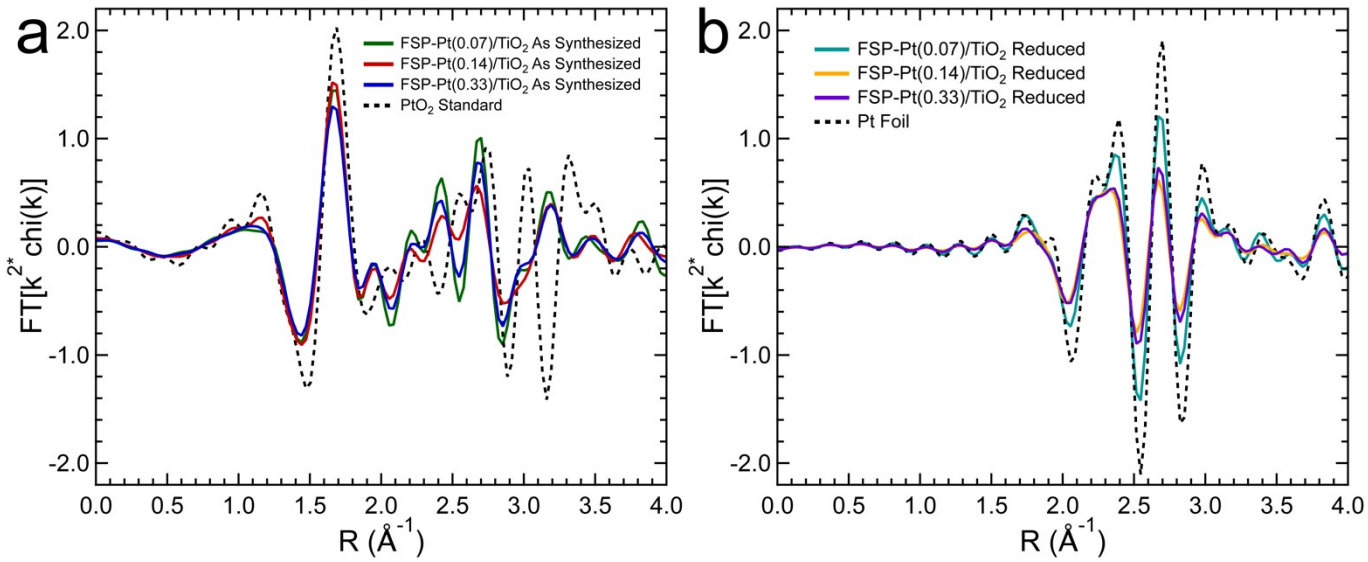

Figure S7. Real component of the Fourier transformed k^2-weighted EXAFS of (a) the as-synthesized and (b) reduced FSP catalysts compared to PtO_2 and Pt foil standards, respectively.

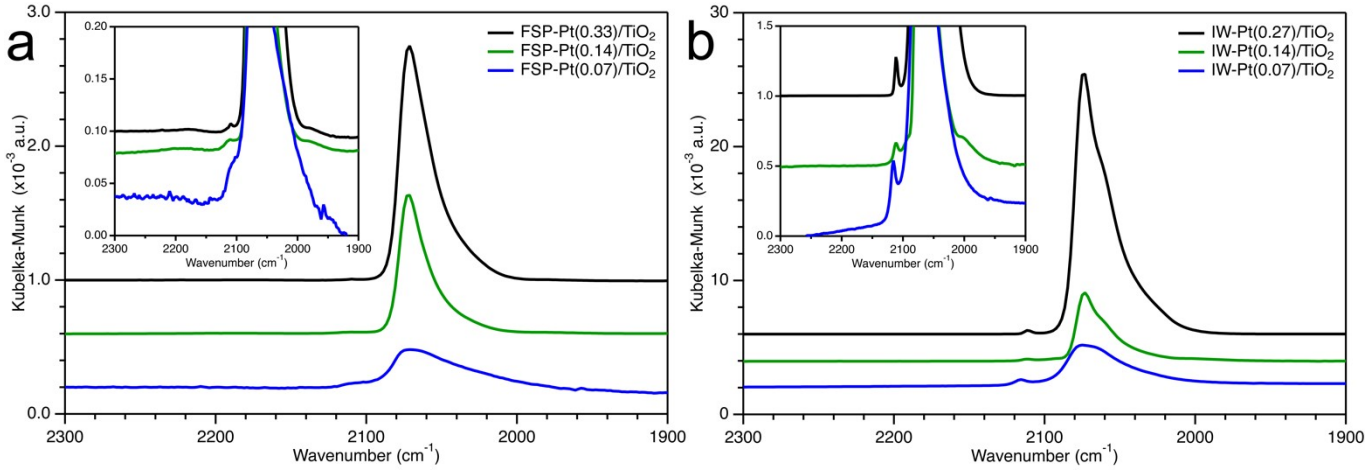

Figure S8. DRIFTS spectra of CO adsorbed on (a) FSP-Pt/TiO_2 and (b) IW-Pt/TiO_2 with magnified insets.

Table S4. Pt L_{III} XANES energies and EXAFS fitting parameters of Pt/TiO_2 catalysts synthesized by flame spray pyrolysis of as-synthesized samples and after reduction in flowing H_2 at 450 °C.

Sample	Edge Energy (eV)	Coordination Number†	R (Å)	σ^2 (x10^3 Å^2)	E_0 (eV)
FSP-Pt(0.07)/TiO_2 As-synthesized	11564.8	3.4 ± 0.4 (Pt-O)	1.99 ± 0.02	1.7 ± 0.7 ‡	11.2 ± 2.4
FSP-Pt(0.07)/TiO_2 Reduced	11562.8	9.2 ± 0.5 (Pt-Pt)	2.75 ± 0.01	5.4 ± 0.2	7.7 ± 0.4
FSP-Pt(0.14)/TiO_2 As-synthesized	11564.4	3.7 ± 0.3 (Pt-O)	1.99 ± 0.01	1.7 ± 0.7 ‡	9.1 ± 1.7
FSP-Pt(0.14)/TiO_2 Reduced	11562.8	7.7 ± 0.6 (Pt-Pt)	2.74 ± 0.01	7.6 ± 0.4	7.8 ± 0.6
FSP-Pt(0.33)/TiO_2 As-synthesized	11564.4	3.2 ± 0.2 (Pt-O)	1.99 ± 0.01	1.7 ± 0.7	9.1 ± 1.4
FSP-Pt(0.33)/TiO_2 Reduced	11562.8	7.7 ± 0.5 (Pt-Pt)	2.75 ± 0.01	6.8 ± 0.4	7.2 ± 0.6
Pt Foil	11562.76	12 (0.86 ± 0.03)	2.76 ± 0.01	4.9 ± 0.2	8.0 ± 0.3
PtO_2	11565.1	6	1.99	---	---

† The amplitude reduction factor (S_0^2) was determined to be 0.86 from the metal foil. This value was fixed for fits of the samples to determine coordination numbers.

‡ As-synthesized catalysts were assumed to contained the same species, but in different amounts. Spectra for as-synthesized materials were fit simultaneously using a single σ^2 while allowing the coordination numbers, bond lengths, and energy shifts to vary.

Table S5. Hydrocarbon product categories for whole biomass vapor upgrading and the corresponding compounds for each as utilized in this work.

Product Categories	Representative molecules
Alkanes	Cycloalkanes (C6-C9), isoalkanes (C5-C8), n-alkanes (C2-C10)
Alkene	Cycloalkenes (C6-C9), isoalkenes (C5-C8), n-alkenes (C2-C10)
Aromatics	1-ring aromatics (benzene, toluene, xylene, ethylbenzene, propylbenzene, methylbenzene), 2-ring aromatics (biphenyl, indane, indene, naphthalene, tetralins), 3-ring aromatics
Partially upgraded Oxygenates	2-butanone, acetone, cyclopentanones, other ketones, phenols, furan
Primary oxygenates	Furanones, methoxyphenols, acetaldehyde, other aldehydes, acids
Unknown	-

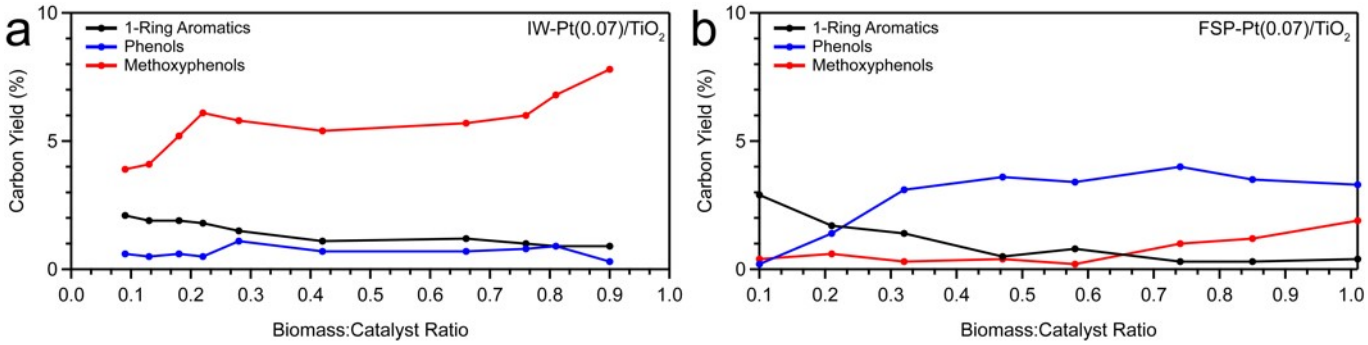

Figure S9. Carbon yield to 1-ring aromatics, phenols, and methoxyphenols as a function of biomass:catalyst ratio for (a) IW-Pt(0.07)/TiO_2 and (b) FSP-Pt(0.07)/TiO_2 catalysts.

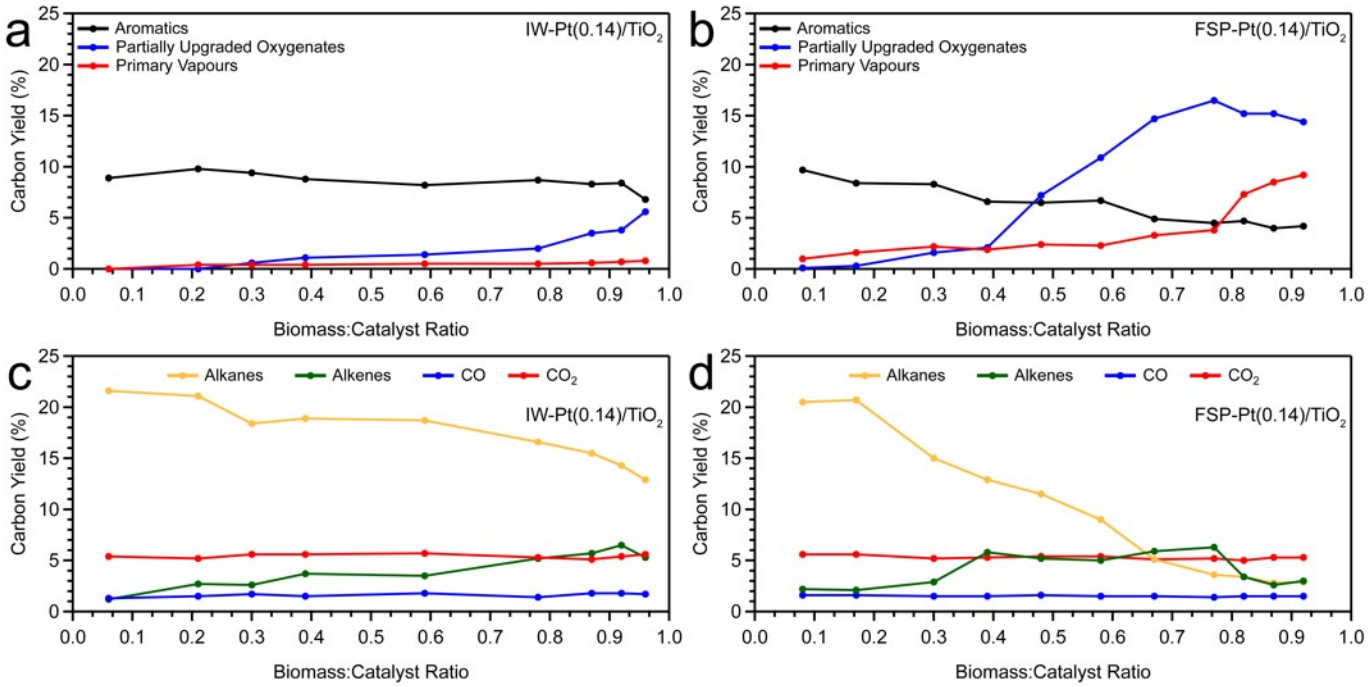

Figure S10. Carbon yield to aromatics, partially upgraded oxygenates, and primary vapours as a function of biomass:catalyst ratio for (a) IW-Pt(0.14)/TiO_2 and (b) FSP-Pt(0.14)/TiO_2 catalysts and carbon yield to alkenes, alkanes, CO, and CO_2, as a function of biomass:catalyst ratio for (c) IW-Pt(0.14)/TiO_2 and (d) FSP-Pt(0.14)/TiO_2 catalysts.

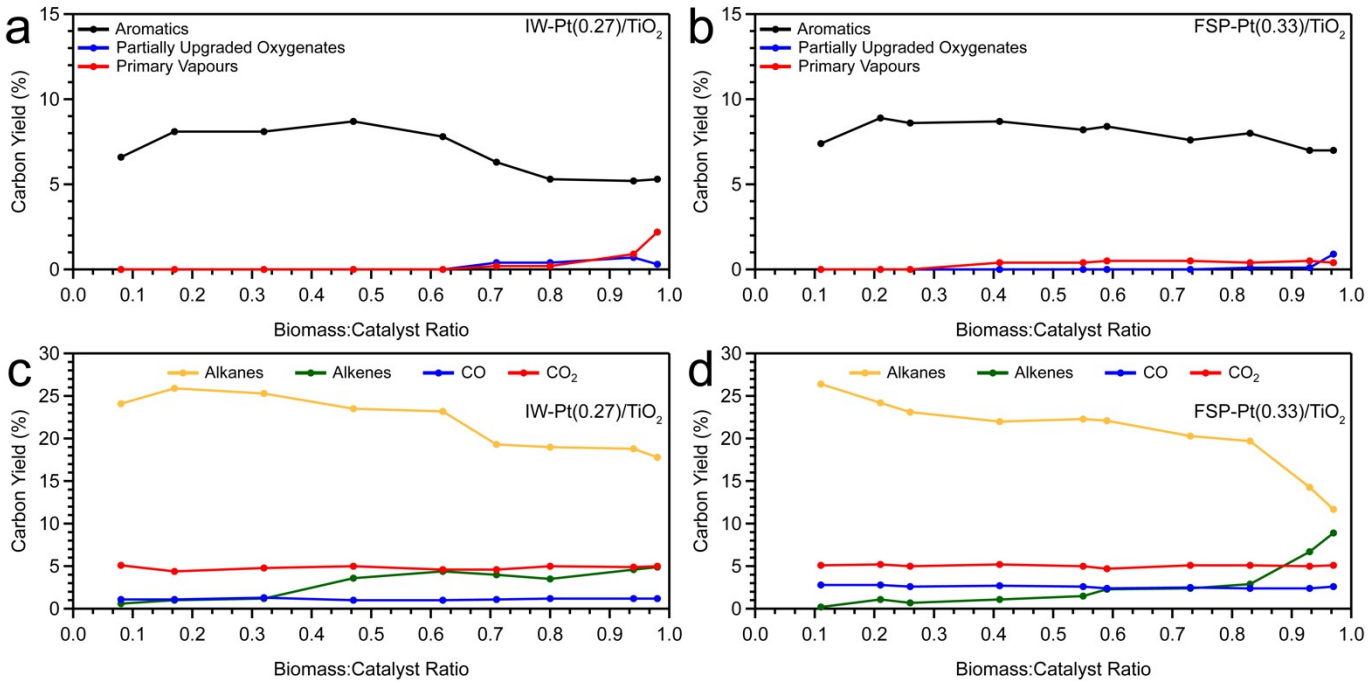

Figure S11. Carbon yield to aromatics, partially upgraded oxygenates, and primary vapours as a function of biomass:catalyst ratio for (a) IW-Pt(0.27)/TiO_2 and (b) FSP-Pt(0.33)/TiO_2 catalysts and carbon yield to alkenes, alkanes, CO, and CO_2, as a function of biomass:catalyst ratio for (c) IW-Pt(0.27)/TiO_2 and (d) FSP-Pt(0.33)/TiO_2 catalysts.